RM E53C26

NACA

RESEARCH MEMORANDUM

DE-ICING AND RUNBACK CHARACTERISTICS OF THREE CYCLIC ELECTRIC, EXTERNAL DE-ICING BOOTS EMPLOYING CHORDWISE SHEDDING

By Robert S. Ruggeri

Lewis Flight Propulsion Laboratory
Cleveland, Ohio

NATIONAL ADVISORY COMMITTEE
FOR AERONAUTICS

WASHINGTON

May 25, 1953

NATIONAL ADVISORY COMMITTEE FOR AERONAUTICS

RESEARCH MEMORANDUM

DE-ICING AND RUNBACK CHARACTERISTICS OF THREE CYCLIC, ELECTRIC, EXTERNAL DE-ICING BOOTS EMPLOYING CHORDWISE SHEDDING

By Robert S. Ruggeri

SUMMARY

An icing investigation was conducted in the Lewis icing research tunnel to determine the general de-icing and runback characteristics of three production samples of electric rubber-clad cyclic de-icing boots. The boots were all designed for the same jet airplane and, hence, were of the same type and were designed to operate at the same values of power density, heat-on time, and cycle ratio. The basic differences among the various boots were in the arrangement and construction of the heater-resistance elements. Each boot employed chordwise shedding and contained a parting strip designed for continuous heating.

The over-all de-icing characteristics of two of the boots investigated were quite similar. The de-icing protection afforded by the boot having small unheated areas existing between segments was slightly less than that of the other two boots. The over-all runback characteristics of the boots were similar for the icing conditions under which the performance was evaluated. The critical areas for all boots investigated were the most forward cycled segments on the upper and lower surfaces (located adjacent to the parting strip). While operating at design power densities and at an angle of attack of 2°, the range of free-stream total temperatures at which the icing protection afforded by the various boots became marginal was from 12° to 15° F for an icing condition having a free-stream velocity of approximately 395 feet per second, a liquid-water content of 0.5 to 0.6 gram per cubic meter, and a droplet diameter from 12 to 14 microns.

INTRODUCTION

The NACA Lewis laboratory is currently engaged in a general investigation of cyclic de-icing of airfoils, which includes the study of various heaters and methods of heating the surface susceptible to icing. Cyclic de-icing of airfoils is that method of thermal ice prevention whereby ice is allowed to form on the airfoil for a relatively short period of time; heat is then applied at a rate sufficient to melt the bond between the ice and the airfoil surface and allow aerodynamic

forces to remove the ice. Upon ice removal, heat is discontinued and the surface is allowed to cool and again to accumulate ice. The cycle is repeated at regular intervals. The principal advantage of the cyclic system over the continuously heated system is the large saving realized in over-all input power requirements (ref. 1).

Inasmuch as previous NACA cyclic de-icing studies (refs. 2 and 3) have all employed models designed specifically for research purposes, this icing investigation was conducted to determine the icing-protection performance and runback characteristics of three samples of actual production de-icing boots. The boots were investigated at two values of angle of attack and free-stream velocity over a range of free-stream total temperatures, liquid-water contents, and droplet sizes.

APPARATUS AND PROCEDURE

Three de-icing boots, which are of the same type but differ considerably in construction and arrangement of heater-resistance elements, were included in the investigation. Although the internal construction of the various boots differs, the boots are all designed to meet the same design and operating specifications. They are of the cyclic, electric, rubber-clad type, and all are designed for the same fighter-type jet airplane. Each boot is 1/8 inch thick (with 0.020-in. rubber over the resistance elements), and each contains a parting strip $1\frac{1}{2}$ inches wide designed for continuous operation at a power density of 13.0 watts per square inch. The design power density for the cycled areas of the various boots is 21.0 watts per square inch. All boots were approximately 28 inches long (spanwise) and extended approximately 12 to 13 inches along the upper and lower surfaces of the airfoil model. A photograph showing two de-icing boots mounted on the airfoil model employed in the investigation is shown in figure 1. Two different boots were mounted simultaneously on the model in order to obtain a better comparison of the performance characteristics of the boots under identical icing conditions.

Whereas previous NACA investigations of cyclic de-icing have all employed models using the principle of spanwise shedding, the boots included in this investigation employed the principle of chordwise shedding of ice. Chordwise shedding differs from spanwise shedding only in the manner in which the cycled portions of the boot are divided into segments. A sketch showing two hypothetical de-icing-boot installations on the wing of the same fighter-type jet aircraft is shown in figure 2. The boot shown in figure 2(a) provides spanwise shedding of ice, whereas the boot installation shown in figure 2(b) provides chordwise shedding.

If the boots are assumed to be comparable in every respect, the boot employing spanwise shedding might operate as follows: Heat is first applied to cycled area 1 (upper and lower surface) for a specified period of time. When heat is discontinued on area 1, it is immediately applied to area 2; proceeding in a spanwise direction until all areas have been heated. For the case of chordwise shedding (fig. 2(b)), the boot is divided into six segments distributed three on the upper and three on the lower surface of the airfoil. Heat might again be applied first to area 1, then to area 2, and so forth, progressing in a chordwise direction across the upper surface of the airfoil and then in like manner across the lower surface.

For purposes of identification throughout this report, the three boots employed in the investigation are labeled A, B, and C, and the cycled segments of each boot are labeled as shown in figure 3. The first letter of the segment notation (A, B, or C) denotes the boot which contains the segment; the second letter (U or L) denotes upper or lower surface; and the number in the segment notation indicates the relative position of the segment with respect to the parting strip. For example, segment BU2 is the second segment of boot B aft of the parting strip on the upper surface of the airfoil.

X-ray photographs showing the internal construction of each boot employed in the investigation are shown in figure 4. The photographs show a small representative area of each boot and are four-fifths scale reproductions of the internal construction of the boots. Boot A (fig. 4(a)) includes a parting strip and six cycled segments evenly distributed around the airfoil. Each segment is approximately $3\frac{7}{8}$ inches wide (chordwise). The solid resistance wires of the cycled segments run in a chordwise direction, that is, parallel to the air flow with the boot mounted on the model. The power leads shown lie beneath the resistance wires with a layer of insulation between the resistance elements and the power leads. The heavy dark areas are bus bars to which the resistance wires are soldered. Approximately 1/8 to 3/16 inch of unheated area exists between the bus bars of adjacent segments of the boot.

Boot B (fig. 4(b)) also consists of a parting strip and six cycled segments, with the segments arranged in a manner very similar to that described for Boot A. All cycled segments are approximately 4 inches wide, with the exception of segments BU3 and BL3, which are 3.1 inches wide. All heater wires, however, are stranded, run in a spanwise direction, and woven into a heavy fabric. Hence, as a result of weaving, when the fabric is sandwiched between two layers of rubber, the resistance wires present a pattern similar to a shallow sine wave in a plane perpendicular to the outer surface of the boot.

Boot C (fig. 4(c)) consists of a parting strip and eight cycled segments, arranged four segments on each side of the parting strip. The segments are approximately $3\frac{1}{8}$ inches wide in the chordwise direction, except segments CU4 and CL4, which are approximately $1\frac{1}{16}$ inches wide for the boot used in the investigation. The solid heater wires are crimped (sine-wave configuration) in a plane parallel to the outer surface of the boot to compensate for dimensional changes due to heating or flexing.

Boots A and C were cured on stainless-steel platens and, hence, possess a smooth and rather glossy surface. Boot B was cured on holland cloth, which resulted in a very fine textured cloth-like appearance of the surface.

The cycling of the boots was accomplished by means of an automatic timer designed to provide a normal cycle ratio of 10 for an individual segment of the cycled areas. The timing for a normal cycle for each segment of a boot was approximately 10-seconds heat-on, 90-seconds heat-off. This timing was changed, however, from time to time during the course of the investigation by manual switching of the timer circuit.

The cycling was identical for the three boots investigated and was done in the following prescribed manner: Cycling began with the application of heat to segment U1 (see fig. 3). The instant heat was terminated on U1, it was applied to U2, and so on, progressing in a chordwise direction across the upper surface of the airfoil. The instant heat was terminated on the most rearward segment on the upper surface, it was applied to segment L1 and progressed across the lower surface. After application of heat to the rearmost segment on the lower surface, cycling was discontinued and ice was allowed to form on the airfoil. The complete cycle was repeated at regular intervals. The parting strip was continuously heated throughout the icing investigation.

The internal circuitry of the boots was quite similar. The circuitry of each segment of each boot (including the parting strip) was arranged in a series-parallel circuit as shown by the schematic diagram presented in figure 5. For boots B and C, several sets of individual heater wires arranged in parallel were wound back and forth spanwise in each segment of the boot. At the spanwise end of each segment, the wires were fastened to electrically conductive strips. In general, the method of construction employed for boot A was similar to that employed for boots B and C, except that in this case, the sets of wires ran back and forth chordwise and were fastened to bus bars which ran in a spanwise direction (see fig. 4). The location of bus bars shown in figure 5 is representative of boots B and C. All segments of the boots were internally connected to a common ground.

The model employed in the icing investigation of the various boots was an NACA 65-213 airfoil section having a 9.3° leading-edge sweepback, an 82.3-inch chord at the center line, and a 71-inch total span. The model is symmetrical about the center line and was mounted vertically in the 6- by 9-foot test section of the icing research tunnel. The airfoil was constructed similarly to an actual wing section of the particular fighter-type jet airplane for which the boots were designed and, hence, incorporated taper in addition to the leading-edge sweepback. A schematic drawing of the model employed in the investigation is shown in figure 6.

The boots were mounted on removable leading edges (1/8-in. aluminum skin) to facilitate installation of the boots. Boot A, which was arbitrarily chosen as a standard for comparison, was mounted on the upper half of the airfoil model (fig. 1). Boots B and C were mounted alternately on the lower portion of the model. A hot-air anti-icing cuff was provided to prevent the formation of ice on the unheated area between the two boots.

The instrumentation of the boots employed in the investigation was rather limited in scope, consisting of only two thermocouples for each segment of a boot. The surface thermocouples consisted of 30-gage iron-constantan wire rolled into ribbons approximately 0.0025 inch thick. The ribbons were butt-welded and laid chordwise over the surface of the boot with the junction located at the approximate center of each segment. Thermocouples were also installed in the aluminum skin underneath the boot at the approximate center of the boot segments.

The performance of the boots was studied for a constant free-stream velocity of approximately 395 feet per second, with the exception of one run that was conducted at a lower free-stream velocity of 288 feet per second. The angles of attack employed were 2° and 6°. The free-stream total temperature was varied from 0° to 25° F, and the liquid-water content from 0.20 to 1.8 grams per cubic meter.

RESULTS AND DISCUSSION

The results presented herein were obtained largely from visual observations and photographs of icing of the various boots. In certain instances, surface-temperature data were obtained in conjunction with the visual and photographic data. Although these temperature data are not available for each test condition investigated, sufficient data are available to evaluate the over-all performance characteristics of the boots.

Boot Surface Temperatures

Typical surface-temperature distributions measured in dry air and in a moderate icing condition for boots A, B, and C are presented in figure 7. The curves were obtained with the boots operating on normal cycle and at design power densities. Normal cycle indicates a heat-on time of approximately 10 seconds and a cycle ratio of 10 for an individual cycled segment of the boot. All temperatures presented in figure 7 are peak temperatures measured at the instant power was discontinued on a particular segment of the boot. Surface temperature is plotted against s/c, where s/c is the ratio of surface distance (measured from the leading edge) to the chord length measured at the planes of instrumentation, expressed in percent. The surface-temperature distribution obtained for each boot operating in dry air at a free-stream total temperature of 15° F, a free-stream velocity of 396 feet per second, and an angle of attack of 2° is presented in figure 7(a). The maximum surface temperature measured for all three boots occurred at values of s/c between zero and 4.0 percent on the lower surface. The minimum surface temperatures occurred on the upper surface of the boots. The variation in surface temperature for each boot ranged from approximately 20° F for boot A to more than 40° F for boot B.

The variation of surface-temperature distribution measured for boots A, B, and C in an icing condition is plotted in figure 7(b). The data shown are for a liquid-water content of 0.57 gram per cubic meter and a droplet diameter of 12 microns. The lowest surface temperature measured in icing occurred at or very near the parting-strip area for each boot. The minimum temperatures are all below 50° F, with the parting strip of boot B reading the lowest value of approximately 43° F. Photographs presented later in the discussion will show that the surface-temperature distributions shown in figure 7(b) did not provide a completely ice-free boot surface for any of the boots investigated in the icing condition listed.

Several curves showing typical variations of measured local surface temperatures with time are presented in figure 8. The time-temperature curves were obtained with the boots operating in an icing condition identical to that presented in figure 7. The curves are presented for various points on the surface of the boots and represent a portion of the data from which the surface-temperature-distribution curves of figure 7 were obtained. The values of s/c listed correspond to the approximate center of the most forward segments, upper and lower surfaces, of the three boots. A comparison of figures 8(a), (b), and (c) shows that the peak surface temperatures measured on the most forward segments of the upper surface of the boots are lowered approximately 10° F by the presence of an icing cloud. This relatively small drop in surface temperature indicates the relatively small amount of impingement and runback occurring over a large portion of the upper surface at an angle of

attack of 2°. Comparison with figures 8(d), (e), and (f) shows that the temperature drop experienced on the lower surface of the boots is about 2.0 to 3.5 times as great as those measured on the upper surface for the values of s/c shown. The irregularities and breaks noted in figures 8(d), (e), and (f) occurred at random intervals and are associated with slow or incomplete shedding of ice, sliding of ice back over the thermocouple junctions, and freezing of water as the surface of the boot falls below the freezing level. For example, the time-temperature curve presented in figure 8(e) shows rapid changes occurring in both the heating and cooling portions of the curve. The abrupt rise in temperature experienced at 6.5 seconds indicates a sudden removal of ice from the surface at that time, while the break noted at 30 seconds is due to the freezing of water on the surface of the boot.

The effect of angle of attack on the surface-temperature distribution for boot A operating in dry air and in icing is shown in figure 9. The temperatures presented are peak values measured at the end of the individual heat-on periods. A considerable change in surface-temperature distribution was observed when the angle of attack was changed from 2° to 6° in dry air, as evidenced in figure 9(a). The largest effect was the change in the temperatures of the parting strip and forward segments on the upper and lower surfaces. The 14° F drop in parting-strip surface temperature is due to the movement of the stagnation point to the lower surface of the airfoil. At high angle of attack, the parting strip has moved so that the local air velocities over it are high, which results in higher convective heat transfer from the surface (the parting-strip surface thermocouple was located at the stagnation point for zero angle of attack).

In an icing condition, increasing the angle of attack from 2° to 6° had practically no effect on the temperature distribution over the upper surface of the boot (fig. 9(b)). The temperatures measured across the lower surface of the boot were higher for the higher angle of attack, while the parting-strip temperature was lowered approximately 5° F by the angle-of-attack increase. For the moderate icing condition listed, the surface-temperature distributions shown in figure 9(b) resulted in essentially complete shedding of ice from the boot surface at both 2° and 6° angles of attack.

The effect of free-stream velocity on the surface-temperature distribution measured for boot A in dry air and in icing is shown in figure 10. For the boot operating in dry air at an angle of 2° (fig. 10(a)), increasing the free-stream velocity from 288 to 397 feet per second resulted in lowered surface temperatures over the entire surface of the boot. The greatest temperature decreases occurred in the area of the parting strip and forward cycled segments. A maximum decrease of approximately 28° F was observed on segment AL1 at an s/c of 2.0 percent.

The variation of the surface-temperature distribution measured in icing for the two values of free-stream velocity is plotted in figure 10(b). The surface temperatures measured at the higher free-stream velocity were all lower than those measured at a free-stream velocity of 288 feet per second, with the exception of segments AU2 and AU3 (upper surface) which were relatively unaffected by the appreciable increase in velocity for the icing condition listed. The maximum decrease in surface temperature occurred on the lower surface at an s/c of approximately 3.0 percent. The surface-temperature distributions shown in figure 10(b) resulted in complete shedding of ice from the heated surface of the boot for both free-stream velocities investigated.

Boot B was used to study the effect of increasing power density (cycled areas) on measured surface-temperature distribution. The variation of surface-temperature distribution for various values of power density and heat-on time is shown in figure 11. The lower dashed curve represents the normal operating conditions for the boot (21.0 w/sq in. for cycled area, 13.0 w/sq in. for parting strip, and a heat-on time of approximately 10 sec). For an icing condition having a free-stream total temperature of 15° F, a free-stream velocity of 395 feet per second, a liquid-water content of 0.55 gram per cubic meter, and a droplet diameter of 12 microns, the normal cycle did not provide complete ice shedding from the surface. Increasing the power density from 21 to 30 watts per square inch and decreasing the heat-on time from 10.2 to 7.0 seconds, thus maintaining a constant input power of approximately 210 watt-seconds to each cycled segment, resulted in higher surface temperatures for all cycled segments, as evidenced by the middle curve presented in figure 11. This more favorable temperature distribution resulted in better shedding characteristics for the boot; however, complete shedding was not attained. Maintaining the power density of 30 watts per square inch and operating the boot at the normal heat-on time of about 10 seconds resulted in the temperature distribution represented by the upper (solid) curve of figure 11. With the boot operating at this over-design condition, complete shedding of ice was attained for each cycle. For the curves shown in figure 11, the parting strip was operated continuously at a power density of 13.0 watts per square inch. Operation at a power density of 30 watts per square inch and a heat-on time of 10 seconds for approximately 30 minutes in the icing condition listed in figure 11 had no apparent detrimental effect on the boot.

Typical variations of local surface temperature measured at a value of s/c of 8.86 percent, upper and lower surfaces, for boot B in icing are shown in figure 12 for several values of power density and heat-on time. The temperatures were measured at the approximate center of segments BU2 and BL2 and in an icing condition identical to that presented in figure 11. In figure 12(b) it can be noted that, for a power density

of approximately 30 watts per square inch, the temperature measured at the center of segment BL2 rose to approximately 32° F even before heat was applied to that segment. This rise was probably due to runback resulting from the application of heat to segment BL1 forward of BL2.

A limited number of temperature measurements made on the aluminum skin beneath the boots showed that the fluctuations of aluminum skin temperatures with time were only of the order of 10° F during the time interval $\left(1\frac{2}{3} \text{ min}\right)$ required for one complete cycle. These rather small fluctuations in skin temperature result from the cycle ratio and heat-on time employed and from the thermal insulating properties of the boots. For a cycle ratio of 10 and a heat-on period of 10 seconds, the residual heat in the boots is not dissipated into the aluminum skin during the short heat-off period of $1\frac{1}{2}$ minutes. Measurements on the upper surface of the airfoil model beneath boot B showed the maximum aluminum skin temperatures to vary almost linearly with s/c from a maximum of 85° F measured beneath the parting strip to a value of 47° F beneath segment BU3 for the following operating conditions: normal cycle, dry air, design power density, free-stream total temperature of 15° F, free-stream velocity of 398 feet per second, and angle of attack of 2°. Skin temperatures measured at isolated points beneath the other two boots indicate that the aforementioned values of skin temperature and temperature fluctuation are typical for all boots investigated.

General De-Icing and Runback Characteristics

The icing and runback characteristics of boots A, B, and C operating with the local surface temperatures and the temperature distributions presented in figures 7 and 8 are shown in figure 13. The photographs show the appearance of the upper surface of the boots after 14 and 22 minutes in the following icing conditions: free-stream total temperature, 15° F; free-stream velocity, 396 feet per second; liquid-water content, 0.57 gram per cubic meter; and angle of attack, 2°. It is apparent that, for these icing conditions, none of the boots provide complete shedding of ice from the surface for operation at design power densities and heat-on time. For longer periods of time in the abovementioned icing condition, the amount of ice adhering to boots B and C remained relatively unchanged, while the amount of ice adhering to boot A increased slightly, which indicated that boot A provides only marginal icing protection for the condition listed. The photographs showing boots A and B indicate the amount of residual ice after the application of heat to segments AU3 and BU3. The photograph of boot C was taken the instant heat was discontinued on segment CU2 and applied to segment CU3. The ice adhering to segments CU3 and CU4 shed clean when heat was applied to these segments.

The photographs shown in figure 13 are typical of the comparative de-icing characteristics of the boots operating in similar icing conditions. In general, for the icing conditions investigated, no appreciable differences in the performance characteristics of boots B and C were observed. Boot B had a fine-textured clothlike surface as compared with the smoother surface of boot C, but this slight difference in surface roughness had little or no effect on ice removal. As evidenced in figure 13, the amount of icing protection afforded by boot A was slightly lower than that of the other two boots; and, hence, the boot provides marginal protection at a slightly higher value of free-stream temperature than does boot B or C, other conditions being equal. In general, for a free-stream velocity of about 395 feet per second, an angle of attack of 2°, and a liquid-water content of 0.5 to 0.6 gram per cubic meter, the range of free-stream total temperatures at which the icing protection afforded by the various boots became marginal was from 12° to 15° F. The slightly lower performance characteristics observed for boot A are attributable to the internal construction of the boot. The presence of rather large bus bars (which act as heat sinks), small unheated areas between all cycled segments, and heater wires running parallel to the airflow at 1/8-inch spacing all contribute to local cold spots from which ice fails to shed during heat-on time. The ice adhering between segments of boot A (fig. 13) is typical of the icing characteristics of the boot. In some cases the ice adhering between segments formed ahead of and behind the small unheated areas between segments to a length of 1 inch or more without adhering to the heated areas. In figure 13(a) it can be noted that considerable ice has formed on the unheated area between the parting strip and the forward cycled segment.

A comparison of figures 13(a), (b), and (c) shows that the runback pattern obtained for the boots in the icing condition listed is quite similar, with no runback occurring on the aluminum skin behind the boot scarf. The runback is a smooth clear ice formation not exceeding 1/8 inch in thickness on the upper surface.

At values of free-stream total temperature of approximately 15° F and less and for velocities of approximately 395 feet per second, the runback was limited essentially to the scarf areas for an angle of attack of 2° and liquid-water contents to 0.6 gram per cubic meter. However, since the boots did not maintain the surface clear of ice at these lower temperatures, the detrimental effect of the small amount of runback is probably slight in comparison with that due to ice accretions observed on the upper surface near the leading edge.

The runback pattern obtained on boots A and B after 56 minutes in icing at a free-stream total temperature of 20° F and a liquid-water content of 0.54 gram per cubic meter is shown in figure 14 for a free-stream velocity of 396 feet per second and a 2° angle of attack. The thickness

of the runback ice shown in figure 14 was about the same for both boots, measuring approximately 1/8 inch thick on the upper surface and 1/4 to 5/16 inch thick on the lower surface. With the boots operating at design power densities and a heat-on time of 11.0 seconds, the heated portion of the boots shed completely clear of ice on each cycle. In general, at the higher tunnel air temperatures and for a free-stream velocity of approximately 395 feet per second, the runback increased in thickness and chordwise extent because of the longer time at which the boot surface remained above the freezing level after a heat-on period.

The runback pattern obtained on boots A and B after 32 minutes of operation in icing at the lowest value of free-stream velocity investigated (288 ft/sec) is presented in figure 15. The runback pattern was obtained in an icing condition having a free-stream total temperature of 20° F, a liquid-water content of 0.66 gram per cubic meter, and a droplet size of 14 microns. The boots were operated at design power density, a heat-on time of 10.0 seconds, and an angle of attack of 2°. The runback pattern and nature of the ice formations observed on the upper and lower surfaces of both boots were found to be very similar. The runback ice was rather clear and smooth. On the lower surface, the runback ice formed a solid sheet approximately 1/4 inch thick for a distance of approximately 3 to 4 inches behind the heated area before changing into a rivulet-like formation which extended back an additional 4 to 8 inches. On the upper surface of the airfoil, the runback ice was approximately 1/8 inch thick with thin rivulet-type ice formations extending as far back as 12 inches behind the heated area.

As can be noted from a comparison of figures 14 and 15, the effect of decreasing speed in a given icing condition is an increase in chordwise extent of runback icing, with a corresponding decrease in runback ice thickness. Although figures 14 and 15 present runback patterns obtained in different icing conditions, the conditions are not so different as to preclude a comparison or an effect due to changes in free-stream velocity.

The runback pattern obtained on the upper and lower surfaces of boots A and C after 32 minutes of operation in an icing condition similar to that presented in figure 14 is shown in figure 16. The runback pattern was obtained in the following icing condition: free-stream total temperature, 20° F; liquid-water content, 0.55 gram per cubic meter; droplet size, 14 microns. The boots were operated at design power densities, a heat-on time of 10.3 seconds, and an angle of attack of 2°. For boot A, runback ice occurred on the aluminum skin behind the boot trailing edge; whereas, for boot C, the runback ice is confined to the scarf area. This apparent difference in runback pattern is probably due to the difference in design of the scarf area of the two boots. The scarf of boot A tapers from 1/8-inch thickness just behind the heated

area to almost a feather edge at the trailing edge of the boot. Boots A and B are designed to be mounted onto the basic airfoil, whereas boot C is designed so that, when mounted on the airplane, the outer surface of the boot is flush with the basic airfoil contour. For this investigation, boot C was cemented onto the leading edge of the airfoil model, and, hence, a sharp step-off of 1/8 inch existed at the trailing edge of the boot. If this difference in trailing-edge design did not exist, it is probable that the runback obtained on boot C would be very similar to that obtained for the other two boots.

In an icing condition for which the free-stream total temperature was 20° F, the free-stream velocity 395 feet per second, and the angle of attack 2°, no secondary buildup of runback ice was observed for operation in clouds composed of droplets whose diameters were less than 15 microns. When larger droplet diameters were employed, direct impingement occurred on the runback ice, and the typical mushroom-ice formations associated with higher-temperature icing were observed on the lower surface behind the heated portion of the boots. At times the mushroom ice attained a height of 2 to $2\frac{1}{2}$ inches before being removed by the aerodynamic forces. For a free-stream total temperature of 25° F and high liquid-water contents, the effective parting strip became very wide, extending at times beyond the center of the forward segments. In addition, in some instances the entire upper or lower surface of the boots was observed to be above the freezing temperature for a short interval of time. During this interval, runback, of course, occurred over the entire surface. Because of the nature of the cooling curves and the manner in which the boots were cycled, the surface temperature of the forward segments did not cool to 32° F before the application of power raised the temperature of the rearmost segments above the freezing value. For example, for boots A and B operating at 10-seconds heat-on time, the surface temperature of segment U3 will exceed 32° F approximately 12 seconds after heat is discontinued on segment U1.

Boots A and B were investigated in an icing condition having a free-stream total temperature of 0° F, a free-stream velocity of 400 feet per second, and a liquid-water content of 0.56 gram per cubic meter. Their icing characteristics in this condition at normal power densities but at approximately 11-seconds heat-on time are shown in figure 17. Photographs were taken after 6 and 22 minutes in the icing condition. Both boots began icing on the forward cycled segments, upper and lower surfaces, from the beginning of the icing exposure. After 15 minutes of icing, the parting strip of each boot was narrowed by approximately 1/2 inch because of the building forward of ice from the cycled area. The parting strip of each boot was completely bridged with ice after 20 minutes in the icing condition. In order to determine the de-icing ability of the boots after leaving an icing condition, the tunnel cloud

was discontinued after 22 minutes while boot power remained on. After 9 minutes of cyclic operation in clear air, no ice was removed from the surface of either boot.

As a result of the icing investigation, it was found that the forward cycled segments, upper and lower surfaces, were the most critical areas for the three boots investigated. Bridging of the parting strip occurred at the more severe icing conditions included in the investigation. In some cases, parting-strip surface temperatures in excess of 75° F were recorded without effecting removal of the ice cap. Although considerable melting occurred beneath the ice cap and the resulting water melted holes through portions of the cap, the inability of the forward cycled segments to melt the bond prevented ice removal.

SUMMARY OF RESULTS

The following results were obtained from an icing investigation of three production samples of electric, cyclic de-icing boots.

1. The forward cycled segments, upper and lower surfaces, of all three boots were the most critical areas for the icing conditions investigated.

2. Unheated areas as small as 1/8 inch wide occurring in the heated surface of an external, rubber-clad, electric, cyclic de-icing boot contributed to local cold spots on which ice forms.

3. The runback characteristics of the three boots were similar.

4. The performance characteristics of two of the three boots were very similar. The icing protection afforded by the boot having small unheated areas existing between segments was slightly less than that of the other two boots.

5. For icing conditions investigated at free-stream total temperature of 15° F and less, the detrimental effect of the small amount of runback ice observed is probably small in comparison with the effect of ice adhering to the surface of the boot just aft of the parting strip because of incomplete shedding.

6. For a free-stream velocity of 395 feet per second and an angle of attack of 2°, the range of free-stream total temperatures at which the icing protection afforded by the various boots became marginal was from 12° to 15° F for the values of liquid-water content included in the investigation.

Lewis Flight Propulsion Laboratory
National Advisory Committee for Aeronautics
Cleveland, Ohio

REFERENCES

1. Gelder, Thomas F., Lewis, James P., and Koutz, Stanley L.: Icing Protection for a Turbojet Transport Airplane: Heating Requirements, Methods of Protection, and Performance Penalties. NACA TN 2866, 1953.

2. Lewis, James P., and Bowden, Dean T.: Preliminary Investigation of Cyclic De-Icing of an Airfoil Using an External Electric Heater. NACA RM E51J30, 1952.

3. Gray, V. H., Bowden, D. T., and von Glahn, U.: Preliminary Results of Cyclical De-Icing of a Gas-Heated Airfoil. NACA RM E51J29, 1952.

Figure 1. - Installation of airfoil model in test section of icing research tunnel.

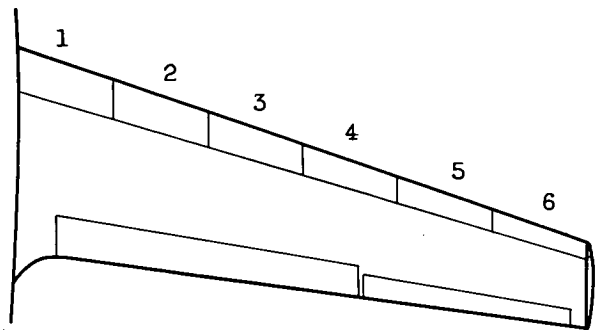

(a) Spanwise shedding.

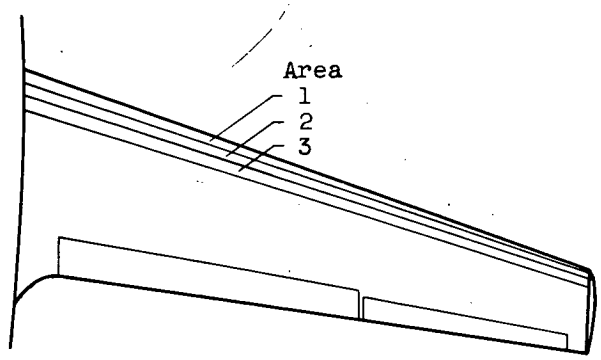

(b) Chordwise shedding.

Figure 2. - Schematic drawing of de-icing-boot installation showing spanwise and chordwise shedding.

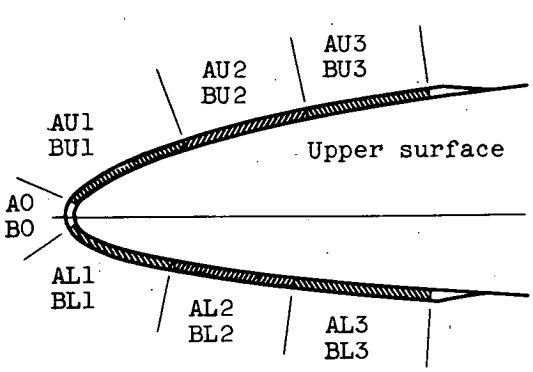

(a) Boots A and B.

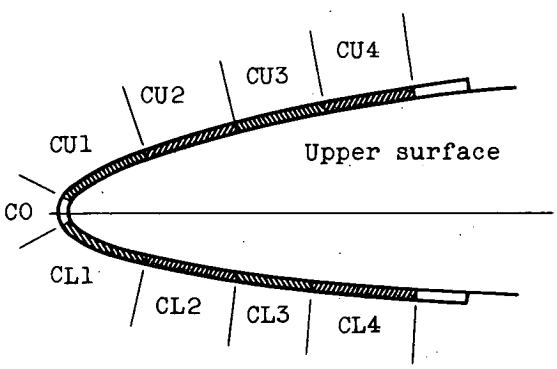

(b) Boot C.

Figure 3. - Segment notation for de-icing boots used in investigation.

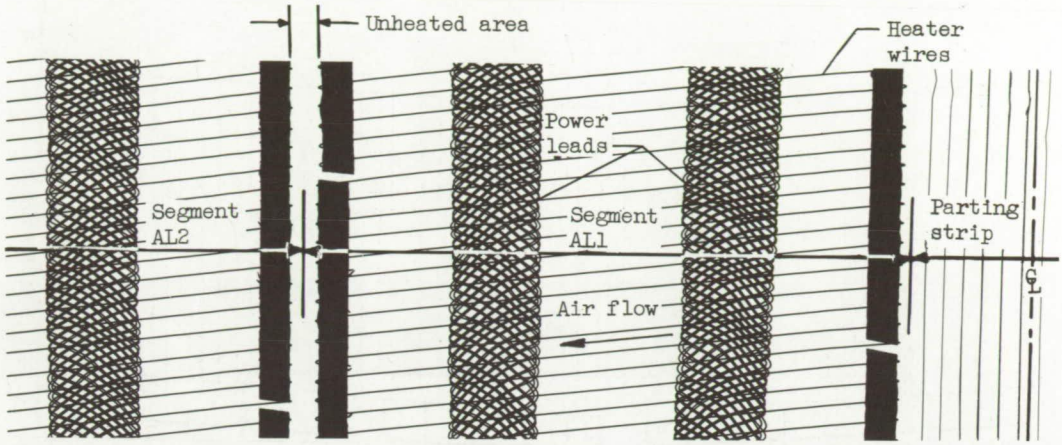

(a) Boot A.

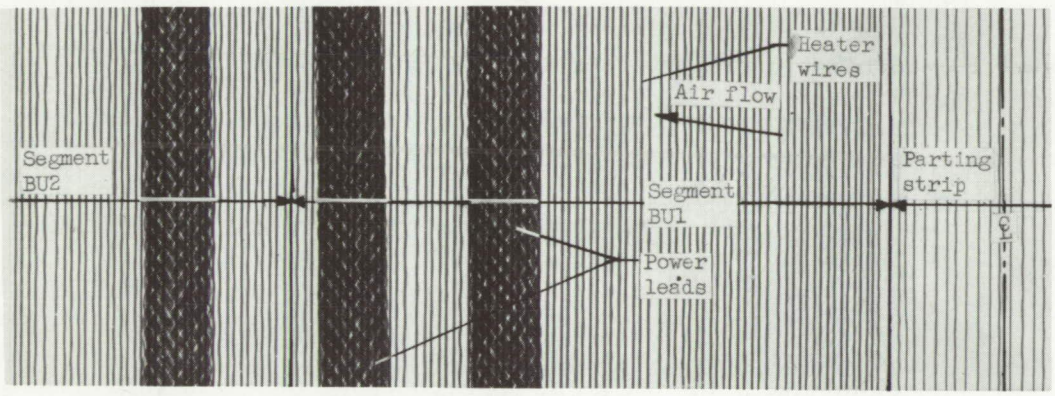

(b) Boot B.

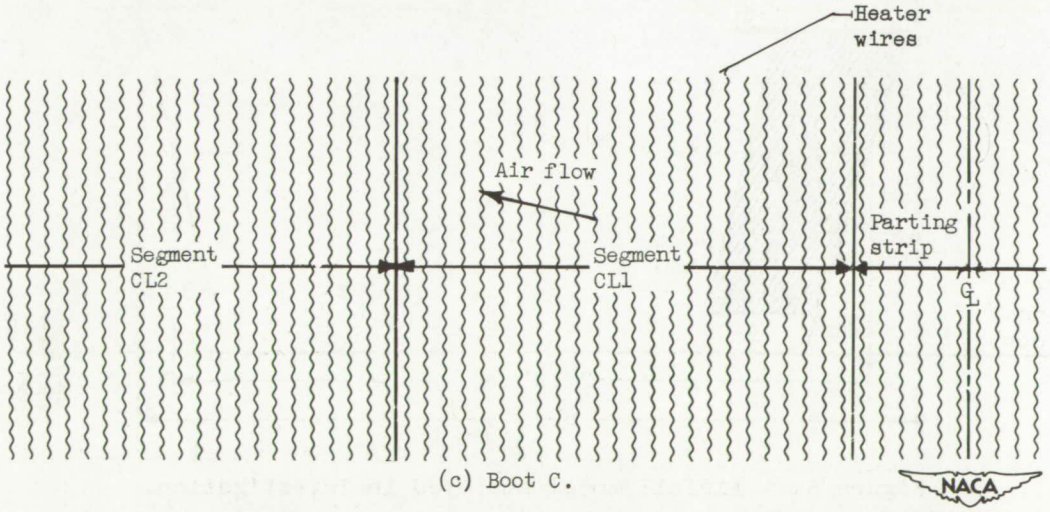

(c) Boot C.

Figure 4. - Internal construction of various boots used in investigation.

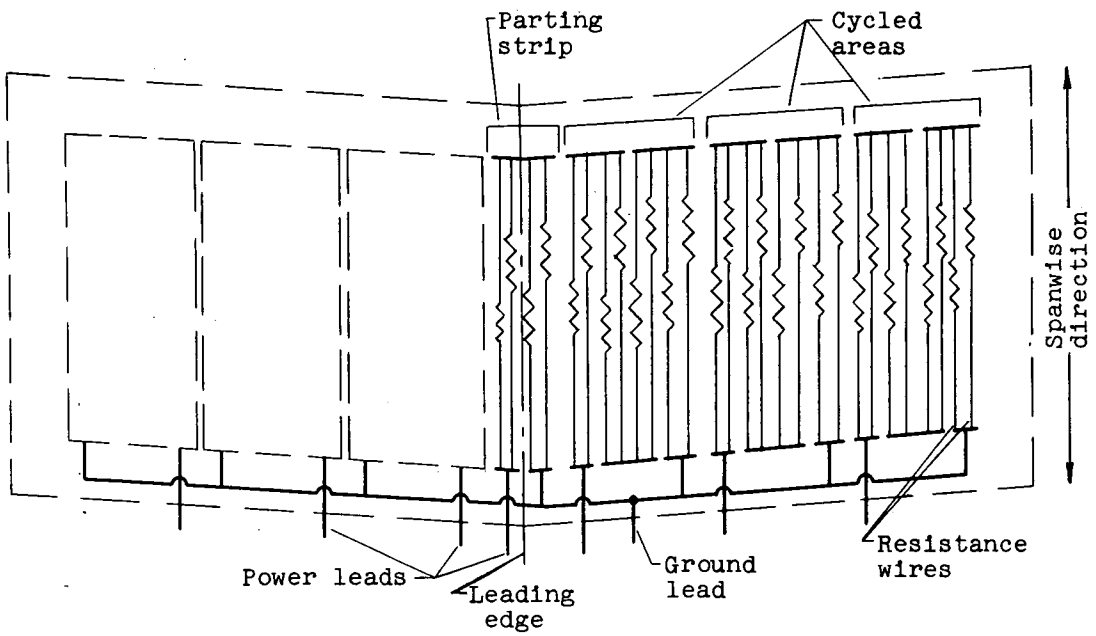

Figure 5. - Schematic diagram showing internal circuitry of boots.

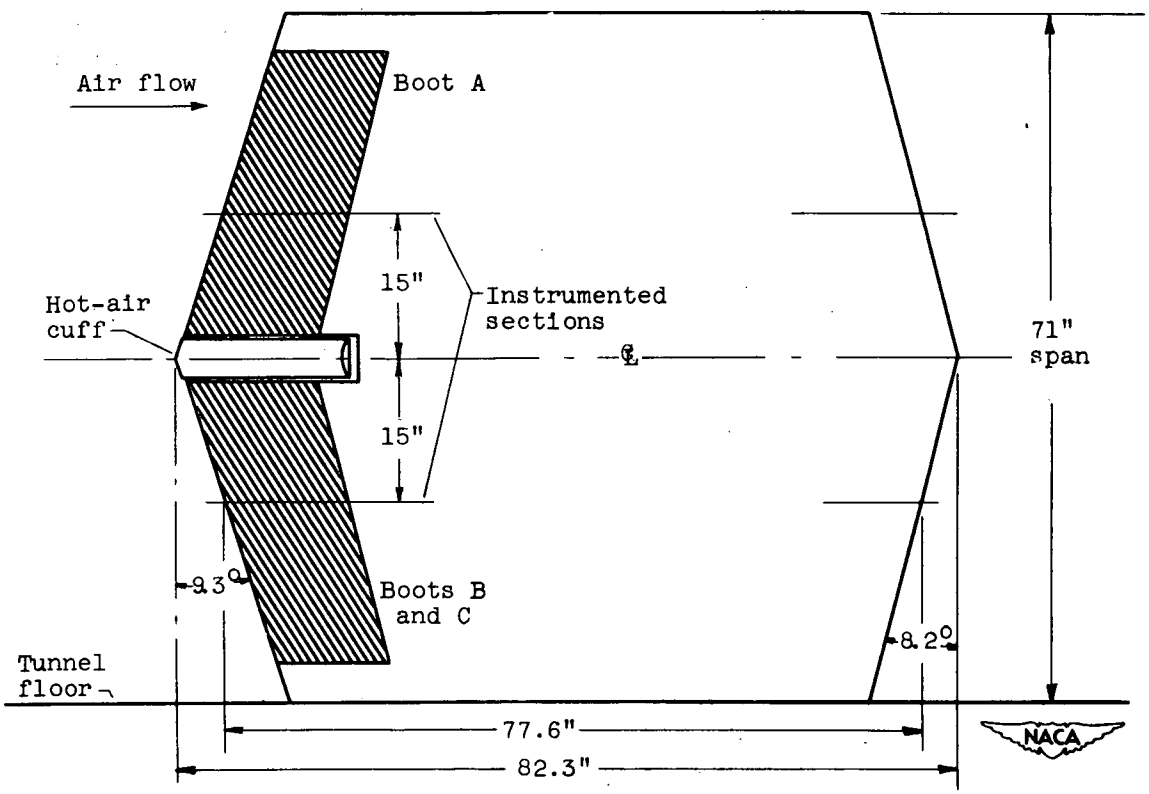

Figure 6. - Airfoil model employed in investigation.

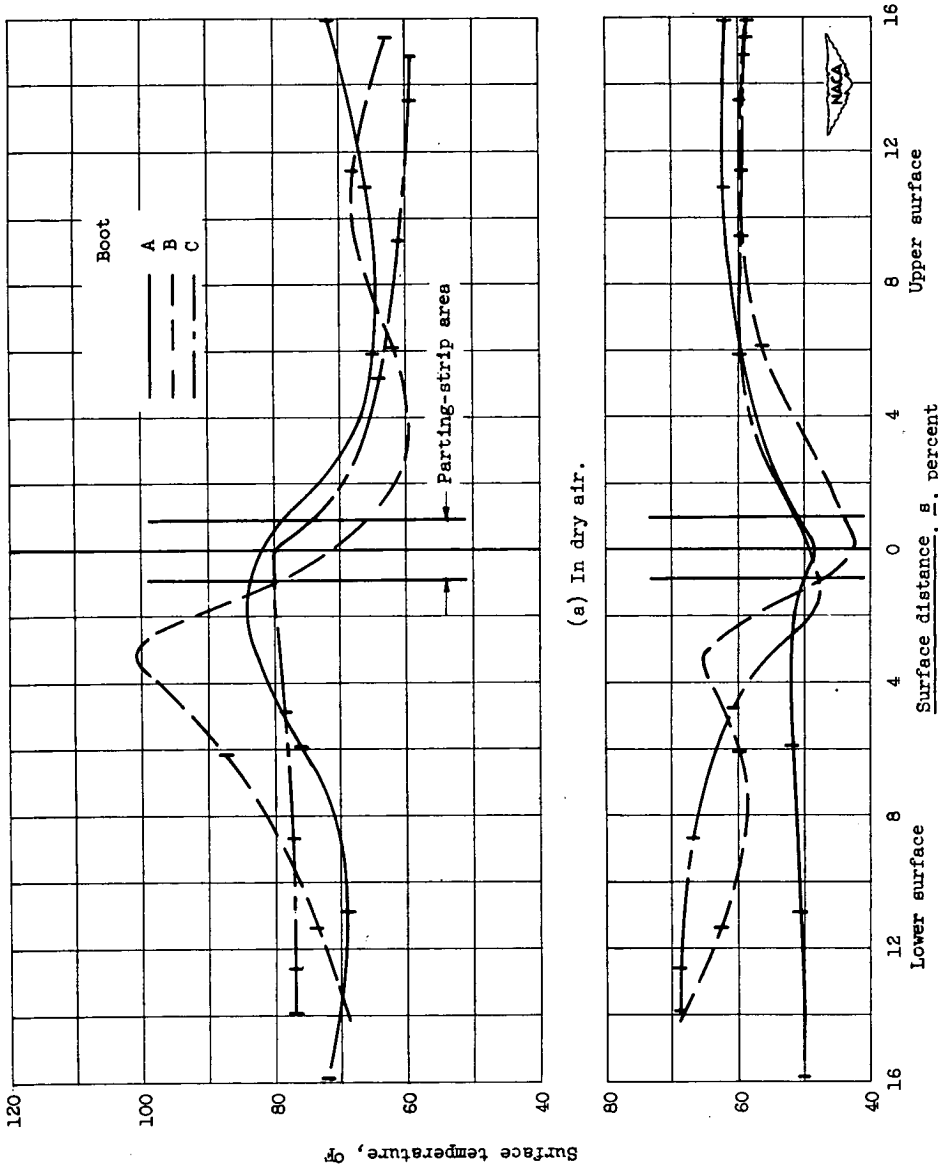

(b) In icing. Liquid-water content, 0.57 gram per cubic meter; droplet diameter, 12 microns.

Figure 7. - Variation of surface-temperature distribution for boots A, B, and C measured in dry air and in icing. Free-stream total temperature, 15° F; free-stream velocity, 396 feet per second; angle of attack, 2°; heat-on time, 10.2 seconds; cycle ratio, 10.

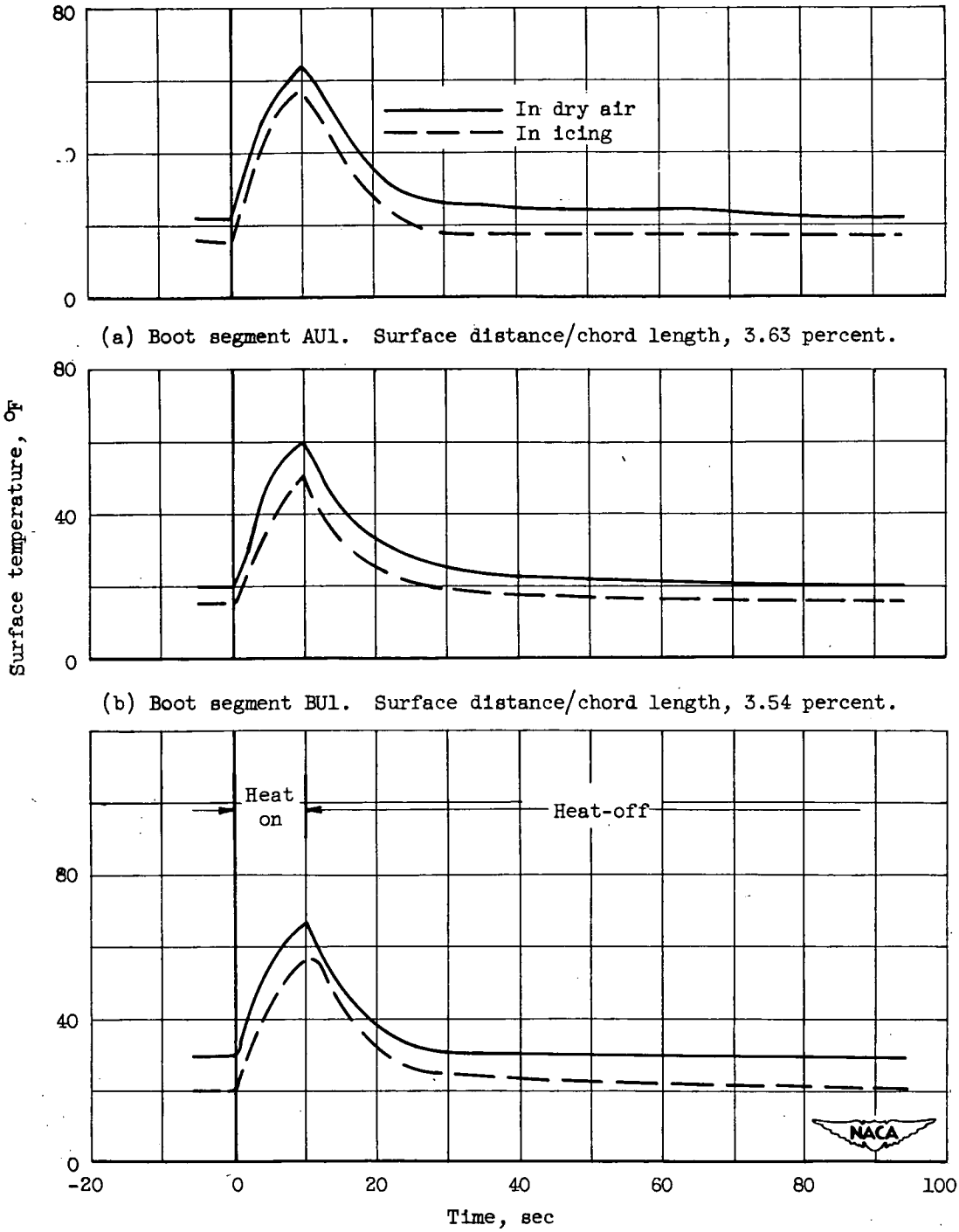

Figure 8. - Typical variation of local surface temperature, upper and lower surfaces, measured in dry air and in icing for three boots. Free-stream total temperature, 15° F; free-stream velocity, 396 feet per second; liquid-water content, 0.57 gram per cubic meter; droplet diameter, 12 microns; angle of attack, 2°; heat-on time, 10.2 seconds; cycle ratio, 10.

(d) Boot segment AL1. Surface distance/chord length, 3.63 percent.

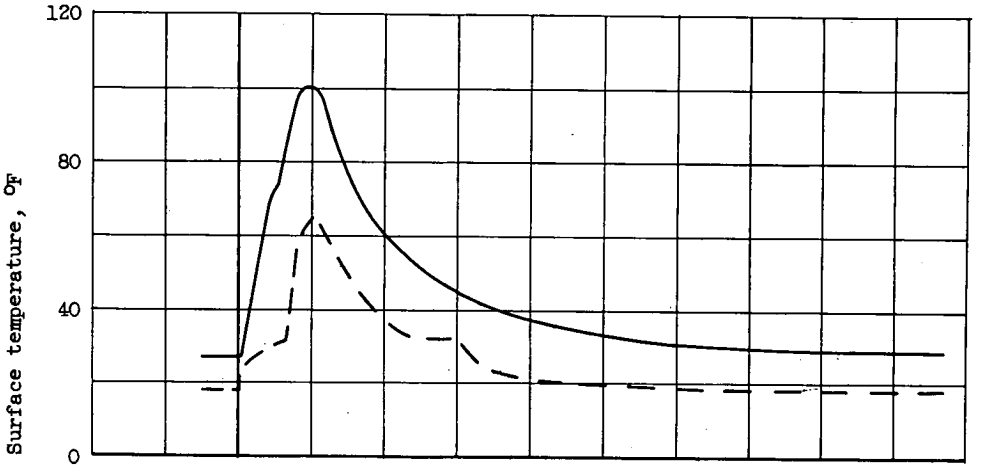

(e) Boot segment BL1. Surface distance/chord length, 3.54 percent.

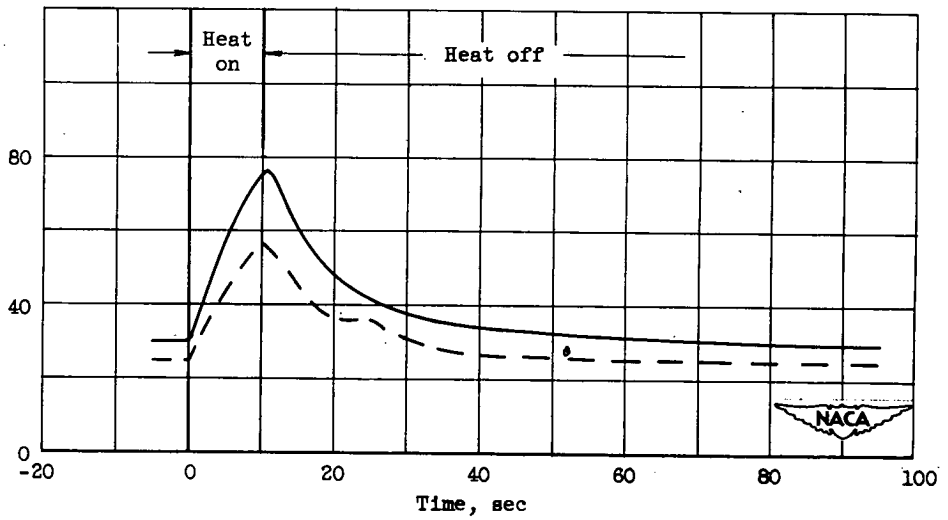

(f) Boot segment CL1. Surface distance/chord length, 2.92 percent.

Figure 8. - Concluded. Typical variation of local surface temperature, upper and lower surfaces, measured in dry air and in icing for three boots. Free-stream total temperature, 15° F; free-stream velocity, 396 feet per second; liquid-water content, 0.57 gram per cubic meter; droplet diameter, 12 microns; angle of attack, 2°; heat-on time, 10.2 seconds; cycle ratio, 10.

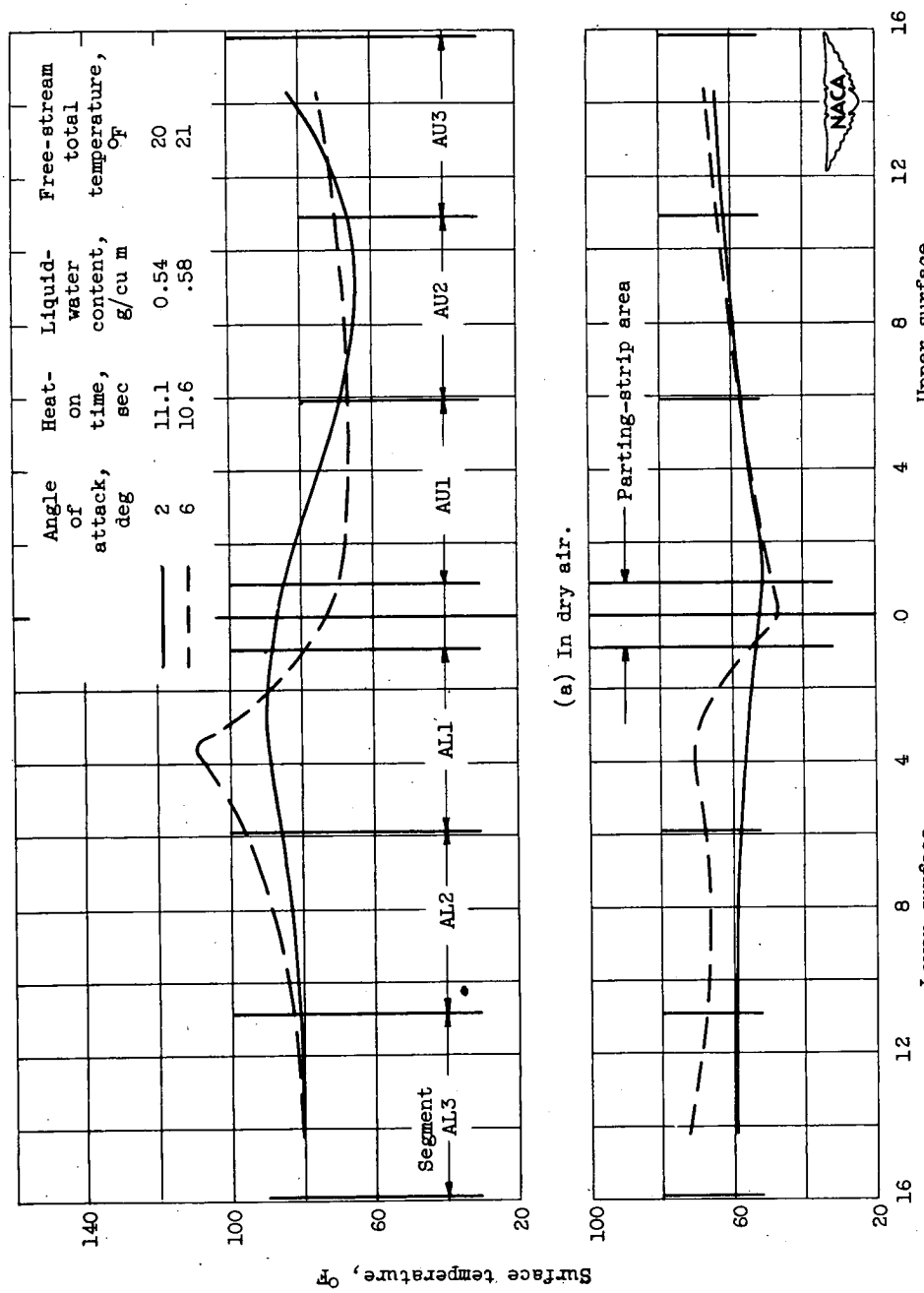

Figure 9. - Effect of angle of attack on surface-temperature distribution in dry air and in icing. Boot A; free-stream velocity, 394 feet per second.

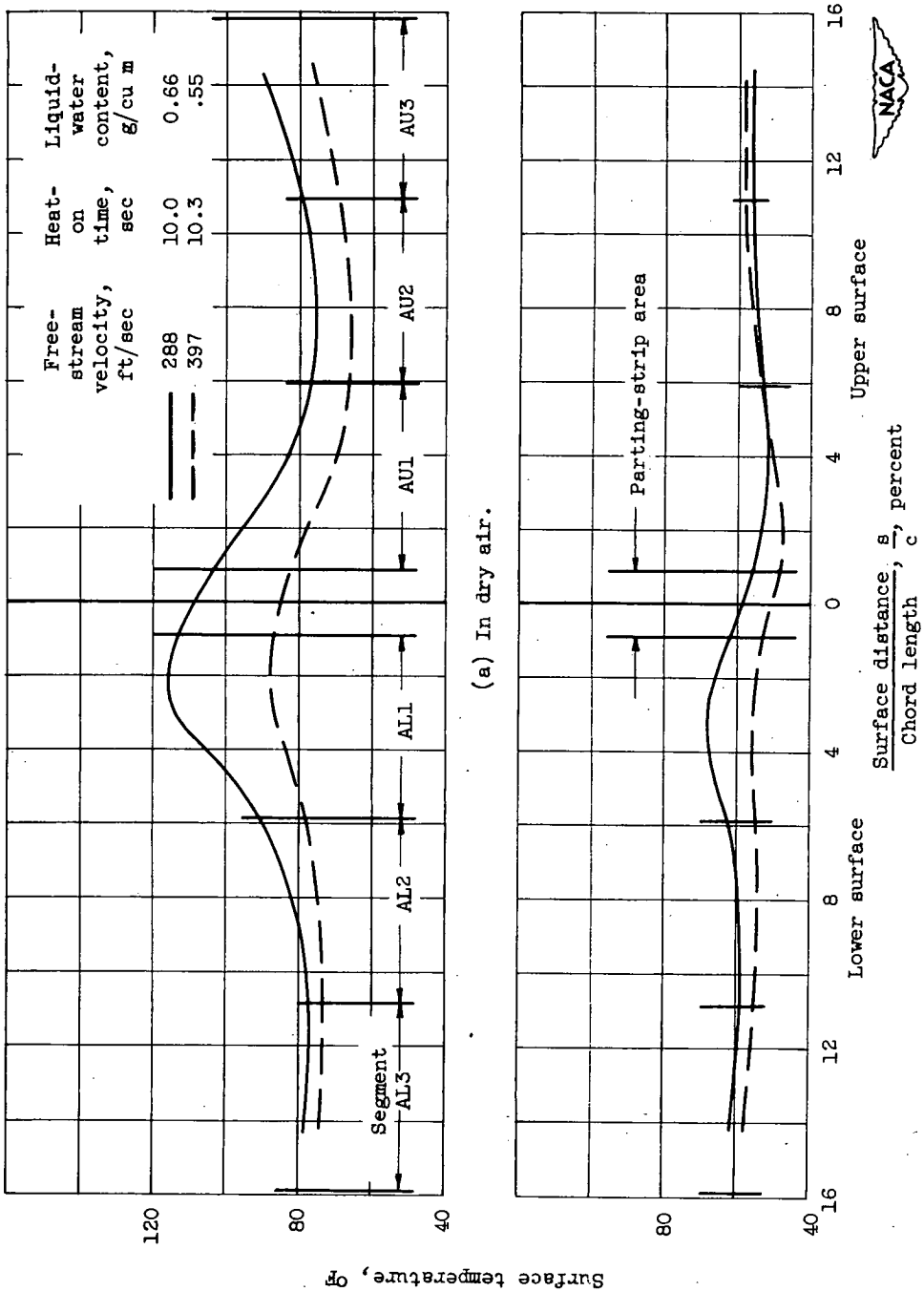

(b) In icing. Droplet diameter, 14 microns.

Figure 10. - Variation of surface-temperature distribution in dry air and in icing for two free-stream velocities. Boot A; free-stream total temperature, 20° F; angle of attack, 2°.

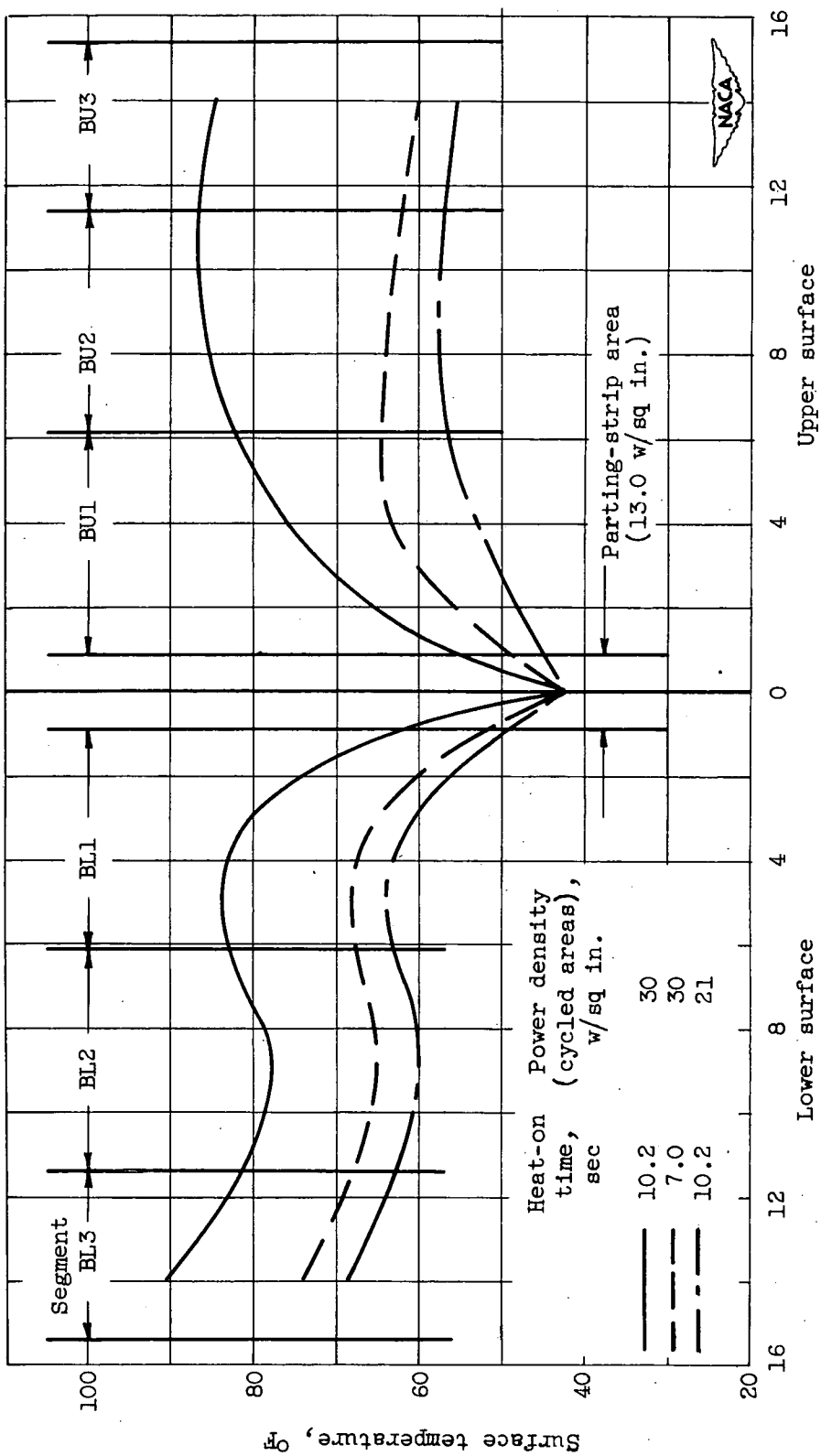

Figure 11. - Variation of surface-temperature distribution measured in icing for various values of heat-on time and power density. Boot B; free-stream total temperature, 15° F; free-stream velocity, 395 feet per second; liquid-water content, 0.55 gram per cubic meter; droplet diameter, 12 microns; angle of attack, 2°.

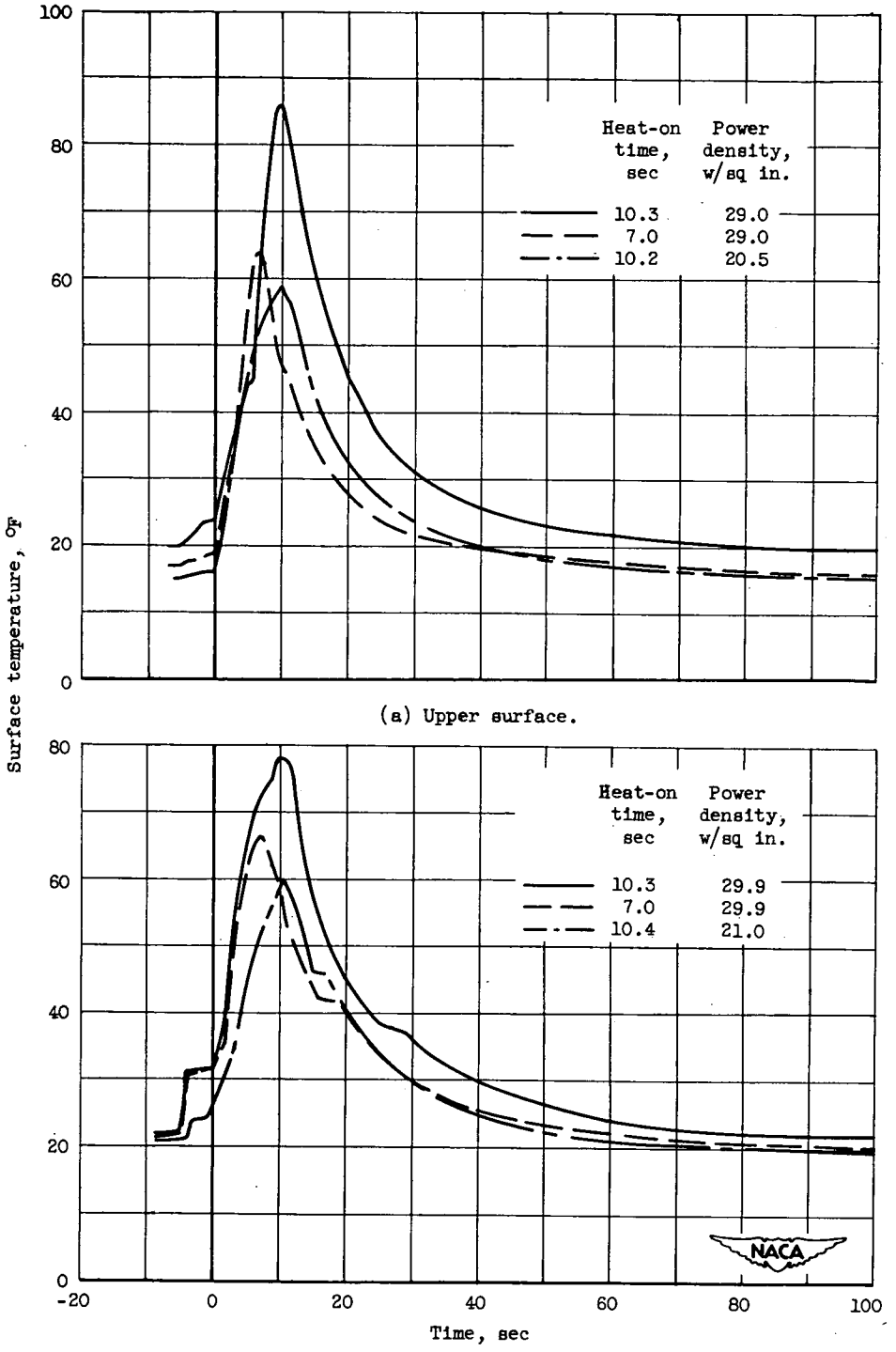

(a) Upper surface.

(b) Lower surface.

Figure 12. - Variation of local surface temperature at s/c value of 8.86 percent, upper and lower surfaces, for various values of heat-on time and power density. Boot B; free-stream total temperature, 15° F; free-stream velocity, 395 feet per second; liquid-water content, 0.55 gram per cubic meter; droplet diameter, 12 microns; angle of attack, 2°.

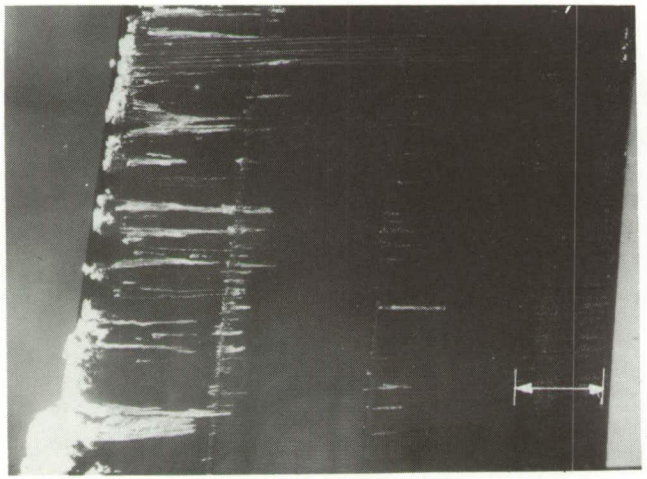

(a) Boot A after 14 minutes in icing.

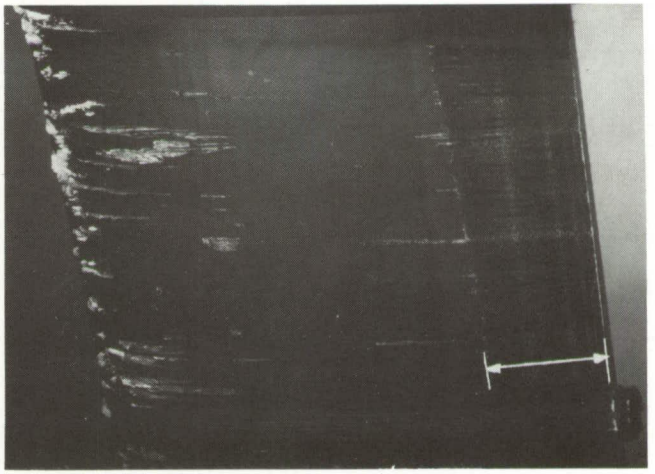

C-30304

(b) Boot B after 14 minutes in icing.

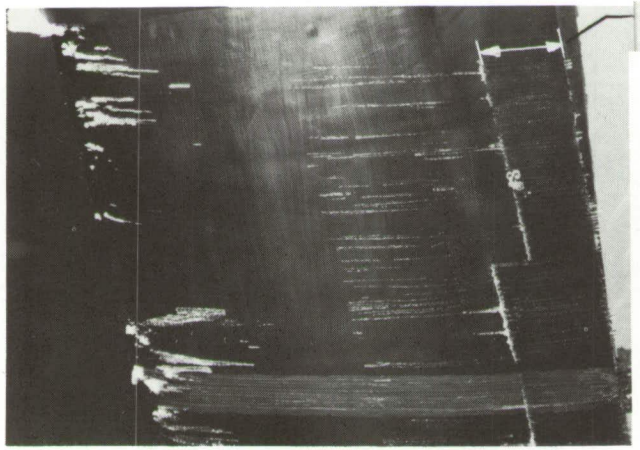

C-30372

(c) Boot C after 22 minutes in icing.

Figure 13. - Appearance of upper surface of boots A, B, and C after several minutes in similar icing conditions. Free-stream total temperature, 15° F; free-stream velocity, 396 feet per second; liquid-water content, 0.57 gram per cubic meter; droplet diameter, 12 microns; angle of attack, 2°; heat-on time, 10.2 seconds; normal power densities.

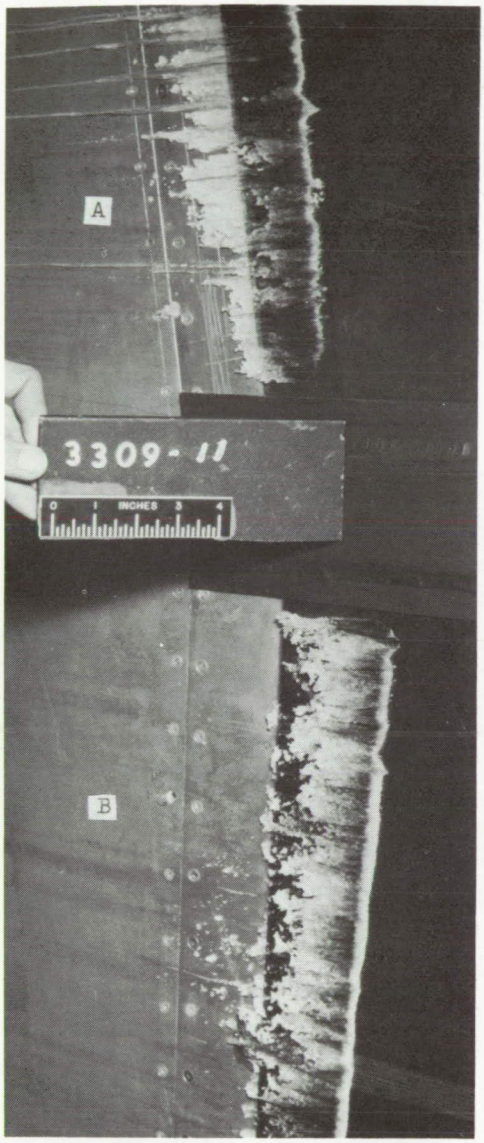

(a) Lower surface.

NACA
C-30276

(b) Upper surface.

NACA
C-30275

Figure 14. - Runback pattern obtained on boots A and B after 56 minutes in icing. Free-stream total temperature, 20° F; free-stream velocity, 396 feet per second; liquid-water content, 0.54 gram per cubic meter; droplet diameter, 12 microns; angle of attack, 2°; heat-on time, 11 seconds; heat-off time, $1\frac{2}{3}$ minutes; normal power densities.

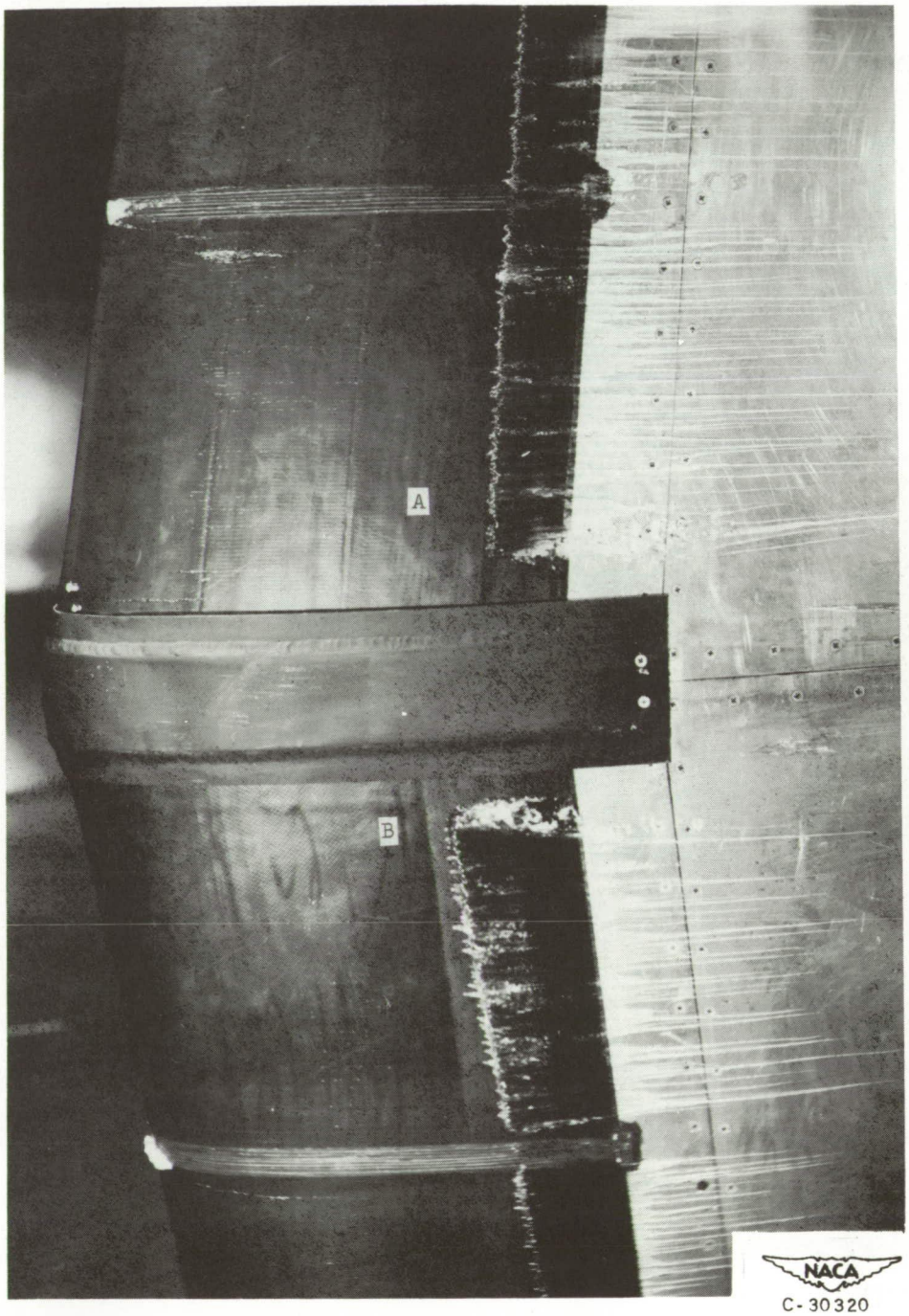

(a) Upper surface.

Figure 15. - Runback pattern obtained on boots A and B after 32 minutes in icing. Free-stream total temperature, 20° F; free-stream velocity, 288 feet per second; liquid-water content, 0.66 gram per cubic meter; droplet diameter, 14 microns; angle of attack, 2°; heat-on time, 10.0 seconds; design power densities.

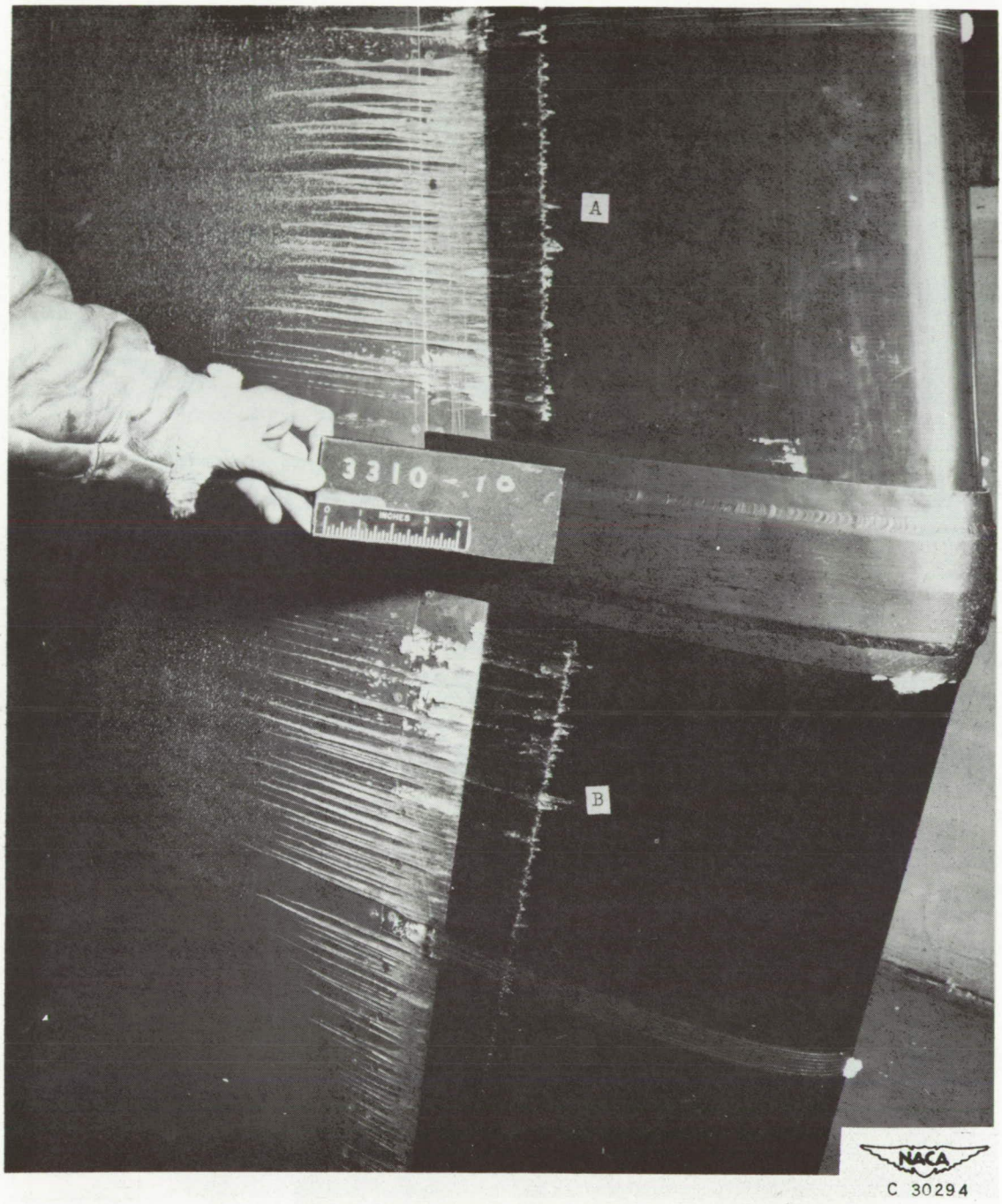

(b) Lower surface.

Figure 15. - Concluded. Runback pattern obtained on boots A and B after 32 minutes in icing. Free-stream total temperature, 20° F; free-stream velocity, 288 feet per second; liquid-water content, 0.66 gram per cubic meter; droplet diameter, 14 microns; angle of attack, 2°; heat-on time, 10.0 seconds; design power densities.

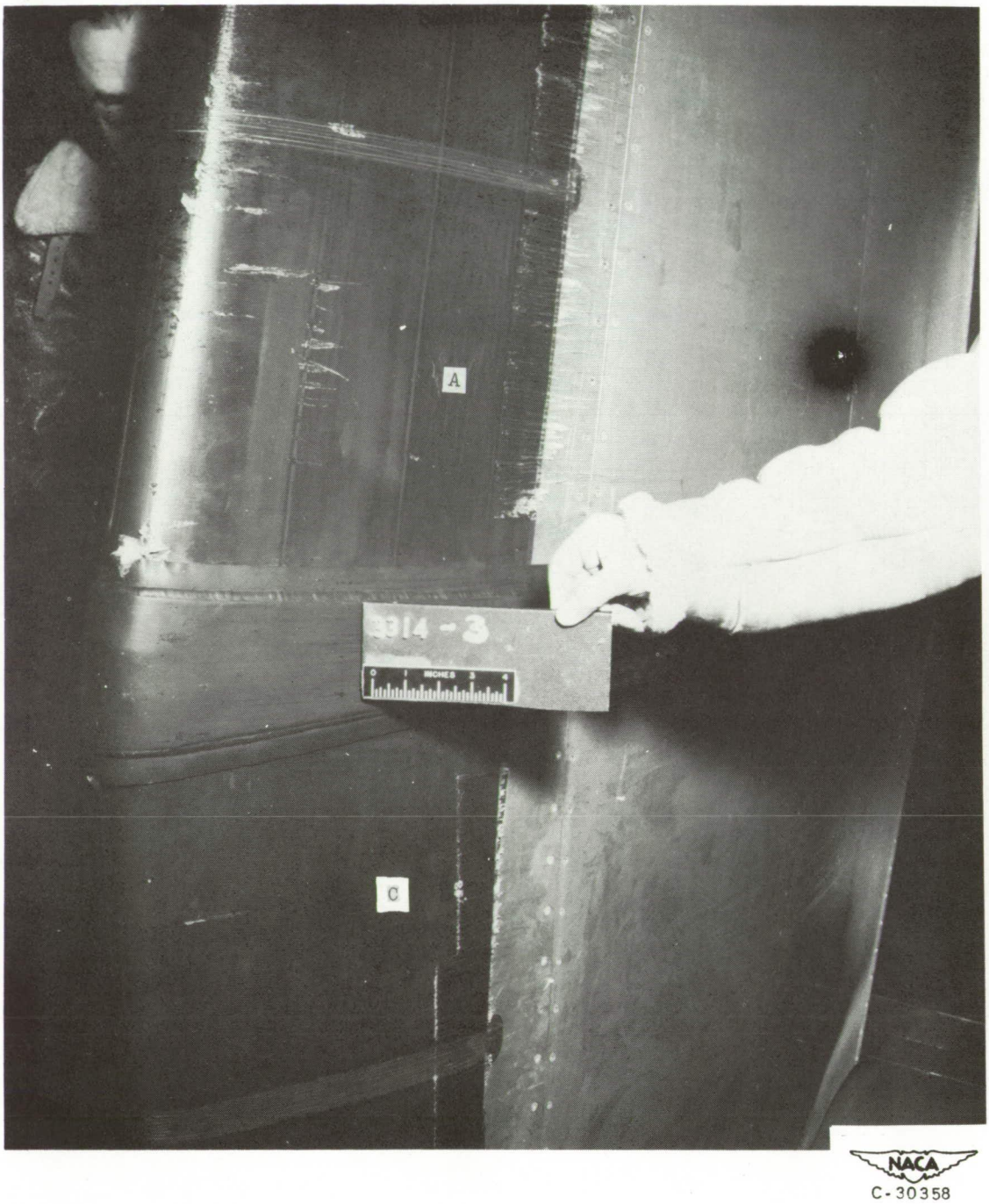

(a) Upper surface.

Figure 16. - Runback pattern obtained on boots A and C after 32 minutes in icing. Free-stream total temperature, 20° F; free-stream velocity, 397 feet per second; liquid-water content, 0.55 gram per cubic meter; droplet diameter, 14 microns; angle of attack, 2°; heat-on time, 10.3 seconds; design power densities.

(b) Lower surface.

Figure 16. - Concluded. Runback pattern obtained on boots A and C after 32 minutes in icing. Free-stream total temperature, 20° F; free-stream velocity, 397 feet per second; liquid-water content, 0.55 gram per cubic meter; droplet diameter, 14 microns; angle of attack, 2°; heat-on time, 10.3 seconds; design power densities.

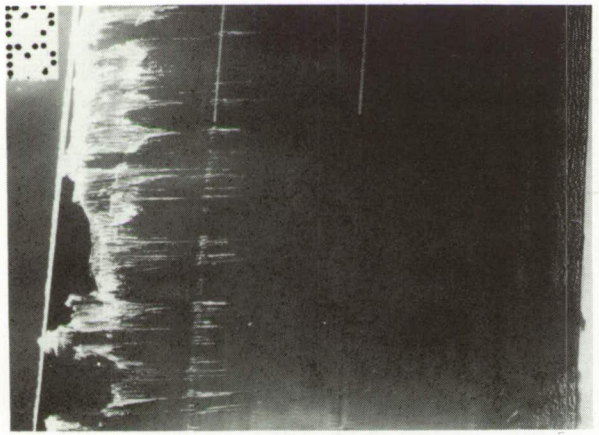

(a) Boot A after 6 minutes in icing.

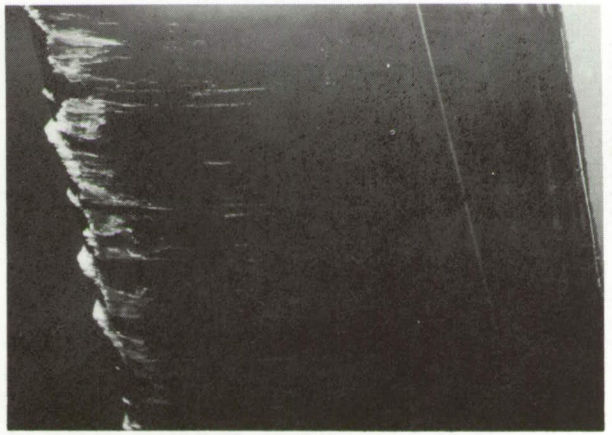

(b) Boot B after 6 minutes in icing.

NACA C-30218

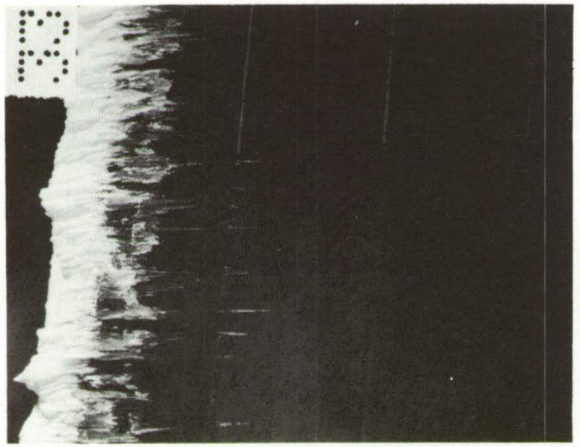

(c) Boot A after 22 minutes in icing.

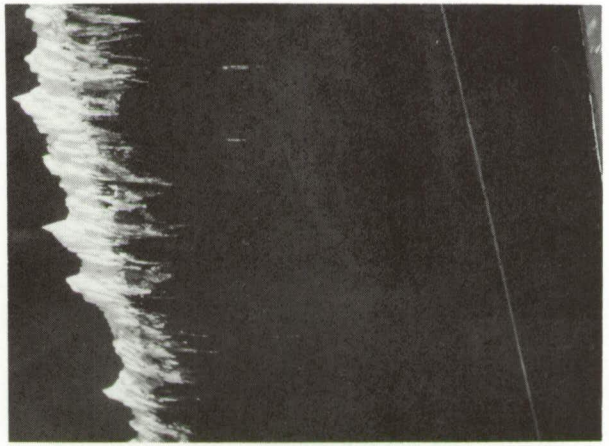

(d) Boot B after 22 minutes in icing.

NACA C-30221

Figure 17. - Appearance of boots A and B after 6 and 22 minutes in icing. Free-stream total temperature, 0° F; free-stream velocity, 400 feet per second; liquid-water content, 0.56 gram per cubic meter; droplet diameter, 10 microns; angle of attack, 2°; heat-on time, 11 seconds; normal power densities.